Lawrence Berkeley National Laboratory

LBL Publications

Title
Nuclear multifragmentation, percolation and the Fisher Droplet model: common features of reducibility and thermal scaling

Permalink
https://escholarship.org/uc/item/89p1w87d

Journal
Physical Review Letters, 85(6)

Author
Elliott, J.B.

Publication Date
2000-02-23

eScholarship.org Powered by the California Digital Library
University of California

LBNL-45102
Preprint

ERNEST ORLANDO LAWRENCE
BERKELEY NATIONAL LABORATORY

Nuclear Multifragmentation, Percolation and the Fisher Droplet Model: Common Features of Reducibility and Thermal Scaling

J.B. Elliott, L.G. Moretto, L. Phair, G.J. Wozniak, S. Albergo, F. Bieser, F.P. Brady, Z. Caccia, D.A. Cebra, A.D. Chacon, J.L. Chance, Y. Choi, S. Costa, M.L. Gilkes, J.A. Hauger, A.S. Hirsch, E.L. Hjort, A. Insolia, M. Justice, D. Keane, J.C. Kintner, V. Lindenstruth, M.A. Lisa, H.S. Matis, M. McMahan, C. McParland, W.F.J. Müller, D.L. Olson, M.D. Partlan, N.T. Porile, R. Potenza, G. Rai, J. Rasmussen, H.G. Ritter, J. Romanski, J.L. Romero, G.V. Russo, H. Sann, R.P. Scharenberg, A. Scott, Y. Shao, B.K. Srivastava, T.J.M. Symons, M. Tincknell, C. Tuvé, S. Wang, P.G. Warren, H.H. Wieman, T. Wienold, and K. Wolf

Nuclear Science Division

February 2000
Submitted to
Physical Review Letters

LOAN COPY
Circulates
For 4 weeks
7th Street Warehouse
Lawrence Berkeley National Laboratory
LBNL-45102
Copy 2

DISCLAIMER

This document was prepared as an account of work sponsored by the United States Government. While this document is believed to contain correct information, neither the United States Government nor any agency thereof, nor the Regents of the University of California, nor any of their employees, makes any warranty, express or implied, or assumes any legal responsibility for the accuracy, completeness, or usefulness of any information, apparatus, product, or process disclosed, or represents that its use would not infringe privately owned rights. Reference herein to any specific commercial product, process, or service by its trade name, trademark, manufacturer, or otherwise, does not necessarily constitute or imply its endorsement, recommendation, or favoring by the United States Government or any agency thereof, or the Regents of the University of California. The views and opinions of authors expressed herein do not necessarily state or reflect those of the United States Government or any agency thereof or the Regents of the University of California.

LBNL-45102

Nuclear Multifragmentation, Percolation and the Fisher Droplet Model: Common Features of Reducibility and Thermal Scaling

J.B. Elliott,[1] L.G. Moretto,[1] L. Phair,[1] G.J. Wozniak,[1] S. Albergo,[2] F. Bieser,[1] F.P. Brady,[3] Z. Caccia,[2] D.A. Cebra,[3] A.D. Chacon,[4] J.L. Chance,[3] Y. Choi,[5] S. Costa,[2] M.L. Gilkes,[5] J.A. Hauger,[5] A.S. Hirsch,[5] E.L. Hjort,[5] A. Insolia,[2] M. Justice,[6] D. Keane,[6] J.C. Kintner,[3] V. Lindenstruth,[7] M.A. Lisa,[1] H.S. Matis,[1] M. McMahan,[1] C. McParland,[1] W.F.J. Müller,[7] D.L. Olson,[1] M.D. Partlan,[3] N.T. Porile,[5] R. Potenza,[2] G. Rai,[1] J. Rasmussen,[1] H.G. Ritter,[1] J. Romanski,[2] J.L. Romero,[3] G.V. Russo,[2] H. Sann,[7] R.P. Scharenberg,[5] A. Scott,[6] Y. Shao,[6] B.K. Srivastava,[5] T.J.M. Symons,[1] M. Tincknell,[5] C. Tuvé,[2] S. Wang,[6] P.G. Warren,[5] H.H. Wieman,[1] T. Wienold,[1] and K. Wolf[4]

[1]Nuclear Science Division
Ernest Orlando Lawrence Berkeley National Laboratory
University of California
Berkeley, California 94720

[2]Universitá di Catania and Istituto Nazionale di Fisica
Nucleare-Sezione di Catania, 95129 Catania, Italy

[3]University of California
Davis, California 95616

[4]Texas A&M University
College Station, Texas 77843

[5]Purdue University
West Lafayette, Indiana 47907

[6]Kent State University
Kent, Ohio 44242

[7]GSI, D-64220 Darmstadt, Germany

February 2000

This work was supported by the Director, Office of Science, Office of High Energy and Nuclear Physics, of the U.S. Department of Energy under Contract No. DE-AC03-76SF00098, and by the National Science Foundation.

Nuclear multifragmentation, percolation and the Fisher Droplet Model: common features of reducibility and thermal scaling

J. B. Elliott[1], L. G. Moretto[1], L. Phair[1], G. J. Wozniak[1],
S. Albergo[2], F. Bieser[1], F. P. Brady[3], Z. Caccia[2], D. A. Cebra[3], A. D. Chacon[4], J. L. Chance[3],
Y. Choi[5], S. Costa[2], M. L. Gilkes[5], J. A. Hauger[5], A. S. Hirsch[5], E. L. Hjort[5], A. Insolia[2], M. Justice[6],
D. Keane[6], J. C. Kintner[3], V. Lindenstruth[7], M. A. Lisa[1], H. S. Matis[1], M. McMahan[1], C. McParland[1],
W. F. J. Müller[7], D. L. Olson[1], M. D. Partlan[3], N. T. Porile[5], R. Potenza[2], G. Rai[1], J. Rasmussen[1],
H. G. Ritter[1], J. Romanski[2], J. L. Romero[3], G. V. Russo[2], H. Sann[7], R. P. Scharenberg[5], A. Scott[6], Y. Shao[6],
B. K. Srivastava[5], T. J. M. Symons[1], M. Tincknell[5], C. Tuvé[2], S. Wang[6], P. G. Warren[5], H. H. Wieman[1],
T. Wienold[1], and K. Wolf[4]
[1] *Nuclear Science Division, Lawrence Berkeley National Laboratory, Berkeley, CA 94720*
[2] *Universitá di Catania and Istituto Nazionale di Fisica Nucleare-Sezione di Catania, 95129 Catania, Italy*
[3] *University of California, Davis, CA 95616*
[4] *Texas A&M University, College Station, TX 77843*
[5] *Purdue University, West Lafayette, IN 47907*
[6] *Kent State University, Kent, OH 44242*
[7] *GSI, D-64220 Darmstadt, Germany*

(February 4, 2000)

It is shown that the Fisher Droplet Model (FDM), percolation and nuclear multifragmentation share the common features of reducibility (stochasticity in multiplicity distributions) and thermal scaling (one-fragment production probabilities are Boltzmann factors). Barriers obtained, for cluster production on percolation lattices, from the Boltzmann factors show a power-law dependence on cluster size with an exponent of 0.42 ± 0.02. The EOS Au multifragmentation data yield barriers with a power-law exponent of 0.68 ± 0.03. Values of the surface energy coefficient of a low density nuclear system are also extracted.

Since the earliest observations of nuclear multifragmentation (the break up of excited nuclei), the Fisher Droplet Model (FDM) [1] and percolation models [2] have been employed in attempts to understand this phenomenon. The FDM enjoyed early success in predicting power-law distributions in fragment masses at the critical point in a liquid-vapor diagram [3]. Percolation models also predicted a power-law distribution in fragment sizes near the critical point [4], [5]. Both models still enjoy great popularity and have been employed in the analysis of Au multifragmentation data obtained by the EOS Collaboration [6], [7], [8], [9], [10].

Other analyses of multifragmentation data have shown two empirical properties of the fragment multiplicities which have been named reducibility and thermal scaling [11], [12], [13], [14]. Reducibility refers to the observation that for each energy bin, E, the fragment multiplicities, N, are distributed according to a binomial or Poissonian law. As such, their multiplicity distributions, P_N, can be *reduced* to a *one-fragment production probability* p, according to the binomial or Poissonian law:

$$P_N^M = \frac{M!}{M!(M-N)!}p^N(1-p)^{M-N};$$
$$P_N = e^{-\langle N\rangle}\frac{1}{N!}\langle N\rangle^N, \qquad (1)$$

where M is the total number of trials in the binomial distribution. The experimental observation that P_N could be constructed in terms of p was considered evidence for stochastic fragment production, *i.e.* fragments are produced independently of each other. Experimental fragment multiplicity distributions were observed to change from binomial to Poissonian under a redefinition of fragment from $3 \leq Z \leq 20$ to individual charges, Z [12].

Thermal scaling refers to the feature that p behaves with temperature T as a Boltzmann factor: $p \propto \exp(-B/T)$. Thus a plot of $\ln p$ vs. $1/T$, an Arrhenius plot, should be linear if p is a Boltzmann factor. The slope B is the one-fragment production barrier. Analyses of multifragmentation distributions along these lines have demonstrated the presence of these features [11] and have led to the extraction of barriers [12]. Controversy has surrounded this type of analysis regarding both the physical existence of these features and their significance, mostly within the framework of dynamical vs. statistical origins of multifragmentation [13].

In this work several important points will be made: The FDM inherently contains reducibility and thermal scaling. Since percolation reduces to the FDM, it exhibits reducibility and thermal scaling. Thus percolation provides a simple mathematical model that fully manifests these two features. Arrhenius plots for percolation can be used to extract barriers. The barriers have a power-law dependence on cluster size. Analysis of the EOS Au multifragmentation data verifies reducibility and thermal scaling. The extracted barriers also obey a power-law dependence on fragment mass.

The FDM and its forerunners [15], [16] are based on the equilibrium description of physical clusters or droplets. The mean number of droplets of size A was written as:

$$\langle N_A \rangle \propto \exp\left[\frac{A\Delta\mu}{T}\right], \tag{2}$$

where $\Delta\mu = \mu - \mu_l$ and μ and μ_l are the actual and liquid chemical potentials respectively. For $\mu < \mu_l$ (gas), $\langle N_A \rangle$ falls to zero with increasing A. For $\mu > \mu_l$ (liquid), $\langle N_A \rangle$ increases with A. To better describe the distribution for intermediate values of A, Eq. (2) was modified to include the surface of the droplets:

$$\langle N_A \rangle \propto \exp\left[\frac{A\Delta\mu}{T} - \frac{c(T)A^{2/3}}{T}\right], \tag{3}$$

where $c(T)$ is the surface free-energy density. For $\mu < \mu_l$, $\langle N_A \rangle$ falls to zero with increasing A. For $\mu > \mu_l$, the terms in the exponential compete, leading to an early decrease in $\langle N_A \rangle$ with A, followed by an increase.

To account for the properties near criticality, Fisher introduced an explicit expression for the surface free energy and a topological factor resulting in an expression for the *normalized* droplet distribution:

$$\langle n_A \rangle = \left\langle \frac{N_A}{A_0} \right\rangle = q_0 A^{-\tau} \exp\left[\frac{A\Delta\mu}{T} - \frac{c_0 \epsilon A^{\sigma}}{T}\right], \tag{4}$$

where: A_0 is the size of the system; q_0 is a normalization constant depending only on the value of τ [17]; τ, the topological critical exponent, depends on the dimensionality of the system with origins that lie in considerations of a three dimensional random walk of a surface closing on itself, for three dimensions $2 \leq \tau \leq 3$; $c_0 \epsilon A^{\sigma}$ is the surface free energy of a droplet of size A; c_0 is the surface energy coefficient; σ is the critical exponent related to the ratio of the dimensionality of the surface to that of the volume; and $\epsilon = (T_c - T)/T_c$ is the control parameter, a measure of the distance from the critical point, T_c.

From this outline it is apparent that the FDM exhibits the features of reducibility and thermal scaling. The distribution in droplet size is Poissonian by construction: in the FDM each component of droplet size A is an ideal gas without the canonical constraint of overall constituent number conservation. The resulting grand canonical distribution is Poissonian. Thus, $\sigma_A^2 = \langle N_A \rangle$, *i.e.* Poissonian reducibility.

Thermal scaling is obvious in the FDM when Eq. (4) is written as follows:

$$\ln\langle n_A \rangle = \ln q_0 - \tau \ln A + \frac{A\Delta\mu}{T} + \frac{c_0 A^{\sigma}}{T_c} - \frac{c_0 A^{\sigma}}{T}. \tag{5}$$

It is clear that linearity with $1/T$ (thermal scaling in an Arrhenius plot) extends to and beyond the critical point, and the slope of the Arrhenius plot gives the $T = 0$ surface energy coefficient of the droplet.

Percolation models are characterized by a constant energy per bond. The bond-breaking probability, p_{break}, is amenable to a straightforward statistical mechanics treatment. Such a treatment reveals that in the limit of $T \to \infty$, $p_{break} \to 1/2$, indicating that the range of p_{break} covered by Eq. (4) is half the usual range discussed in percolation theory; $0 \leq p_{break} \leq 1$. Such a literal thermodynamical treatment therefore excludes the critical point, p_c, of many types of percolation systems from thermodynamic consideration.

However, percolation phenomena, with a geometrical phase transition, share with thermal critical phenomena the important features of *scaling*, *universality* and *renormalization group* as well as other deep connections [18]. For example, the scaling behavior observed in percolation clusters can be described by the FDM when p_{break} replaces T in Eq. (4) and the control parameter becomes $\epsilon = (p_c - p_{break})/p_c$ [2].

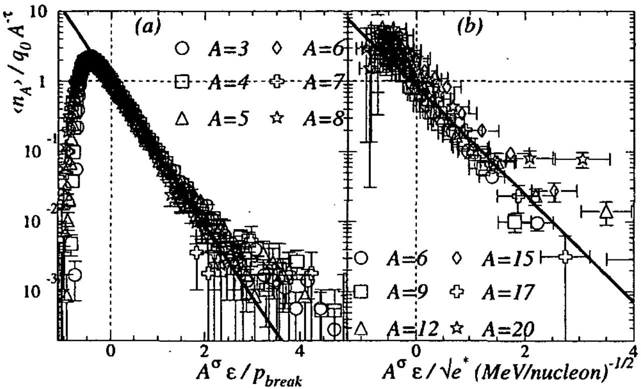

FIG. 1. The scaled cluster (fragment) distribution plotted as a function of the scaled control parameter for clusters (fragments) of size (mass) A. The solid line shows a fit to the FDM for (a) percolation ((b) Au multifragmentation).

To demonstrate the scaling of percolation clusters a plot is made of the scaled cluster distribution, $n_A^{scaled} = \langle n_A \rangle / q_0 A^{-\tau}$, as a function of the scaled control parameter, $\epsilon^{scaled} = A^{\sigma}\epsilon/p_{break}$. See the left panel of Fig. 1. Data over a wide range in A and ϵ are seen to collapse. Cluster distributions used in this analysis were generated on a simple cubic lattice of side six [19].

Fitting n_A^{scaled} as a function of ϵ^{scaled} for $\epsilon \geq 0$ and leaving c_0 and $\exp[A\Delta\mu/p_{break}]$ as free parameters in Eq. (4) gives $c_0 = 2.34 \pm 0.03$ and $\exp[A\Delta\mu/p_{break}] = 0.95 \pm 0.01$, *i.e.* the bulk factor is unity. At the critical point, $\epsilon = 0$, the collapsed distribution takes the value of one indicating that the cluster distribution follows a power law. Away from the critical point, the cluster distribution predominantly follows the surface term in Eq. (4). The FDM does not describe the behavior of clusters for $\epsilon \ll 0$. Other forms for the FDM's surface factor have been suggested to describe cluster behavior on both sides of the critical point [2], [19].

Also shown in Fig. 1 is a plot of the EOS Au multifragmentation data [6], [7], [8], [9], [10]. Here the substitution of $\sqrt{e^*} = \sqrt{E^*/A_0}$ for T has been made resulting in a control parameter of $\epsilon = (\sqrt{e_c^*} - \sqrt{e^*})/\sqrt{e_c^*}$, which for a degenerate Fermi gas reduces to $(T_c - T)/T_c$. The excitation energy normalized to the mass of the fragmenting remnant, e^* in MeV/nucleon, excludes collective effects [9]. The location of the critical point, e_c^*, and values of the critical exponents, σ and τ, were determined previously [6], [7], [8], [9], [10]. Fitting n_A^{scaled} as a function of ϵ^{scaled} for $\epsilon \geq 0$ and leaving c_0 and $\exp\left[A\Delta\mu/\sqrt{e^*}\right]$ as free parameters in Eq. (4) gives $c_0 = 6.4 \pm 0.6$ MeV (via $E^* = aT^2$ with $a = A_0/13$) and $\exp\left[A\Delta\mu/\sqrt{e^*}\right] = 0.8 \pm 0.1$, *i.e.* the bulk term is consistent with $\Delta\mu \approx 0$. The surface energy coefficient c_0 is of a somewhat different nature than the semiempirical mass formula parameter ($a_s \sim 17$ MeV for $T = 0$, $\rho = \rho_0$) or estimates for low density nuclear systems ($a_s \sim 6$ MeV for $T \sim 3$ MeV, $\rho \sim \rho_0/3$) [20]. The coefficient c_0 is temperature independent; the temperature dependence is given as $c_0\epsilon$.

Since the FDM has been shown to contain the features of reducibility and thermal scaling and since the scaling inherent in the FDM describes percolation, it should be possible to observe reducibility and thermal scaling in percolation cluster distributions.

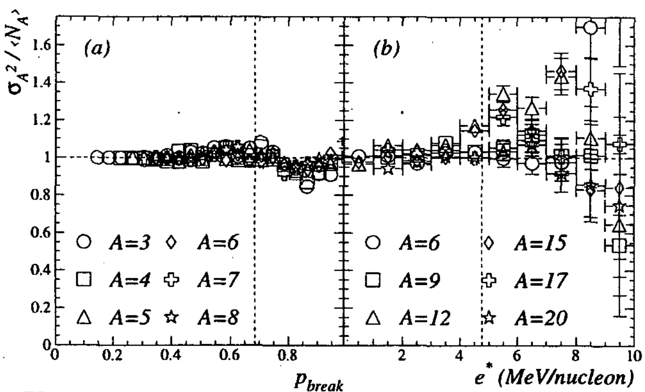

FIG. 2. Ratio of the variance to the mean number of clusters (fragments) of size (mass) A as a function of p_{break} (e^*) for percolation (a) (Au multifragmentation (b)). Error bars are statistical. Vertical dashed lines show the location of the critical point.

To address the question of reducibility in percolation, cluster multiplicity distributions for bins in p_{break} are considered. The ratio of the variance to the mean, $\sigma_A^2/\langle N_A\rangle$, of the multiplicity distribution for each cluster of size A is an indicator of the nature of the distribution. In Fig. 2, such a ratio is shown as a function of p_{break}. The observed ratio is near one (Poissonian limit) over the range of p_{break}. Within experimental errors, similar behavior is observed for the Au multifragmentation data.

Examples of multiplicity distributions with Poissonian curves calculated from percolation $\langle N_A\rangle$ are shown in the left panel of Fig. 3. Poissonian distributions reproduce percolation cluster distributions over two or three orders of magnitude for all A values; Poissonian reducibility is present in percolation.

Fig. 3 also shows the multiplicity distributions for Au multifragmentation compared to the calculated Poissonian curves. The agreement between the measured and computed distributions confirms the presence of reducibility in the Au multifragmentation data.

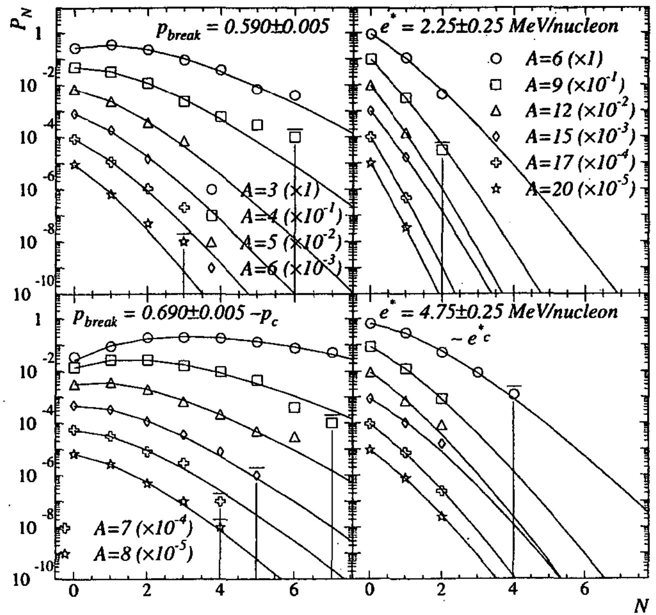

FIG. 3. Multiplicity distributions, P_N, for clusters (fragments) of size (mass) A as a function of N for bins in p_{break} (e^*) for percolation (Au multifragmentation) on the left (right). The lines are Poissonian distributions calculated from the measured $\langle N_A\rangle$.

To verify thermal scaling in percolation, the average yield of clusters of size A and its dependence on p_{break} are considered. The presence of thermal scaling should manifest itself through a Boltzmann factor. Again, the substitution p_{break} for T is made in accordance with standard percolation theory and $\ln\langle n_A\rangle$ is plotted as a function of $1/p_{break}$ (Arrhenius plot). See Fig. 4. In most cases the Arrhenius plots for individual clusters of size A are linear over two orders of magnitude. Thus, thermal scaling is verified for percolation. The observations that reducibility and thermal scaling are already present in such a simple model suggest that they are deeply rooted fundamental features of multifragmentation processes rather than being epiphenomena of complex systems.

The Boltzmann factor indicates that the slope of an Arrhenius plot represents the barrier B associated with the production of a cluster. For an interpretation of B in percolation, the Boltzmann factor is equated with Eq. (4) yielding a power law relating B to the size of a cluster: $B = c_0 A^\sigma$ when $\Delta\mu \approx 0$. Fitting the extracted barriers B (slopes in Fig. 4) as a function of A gives an exponent

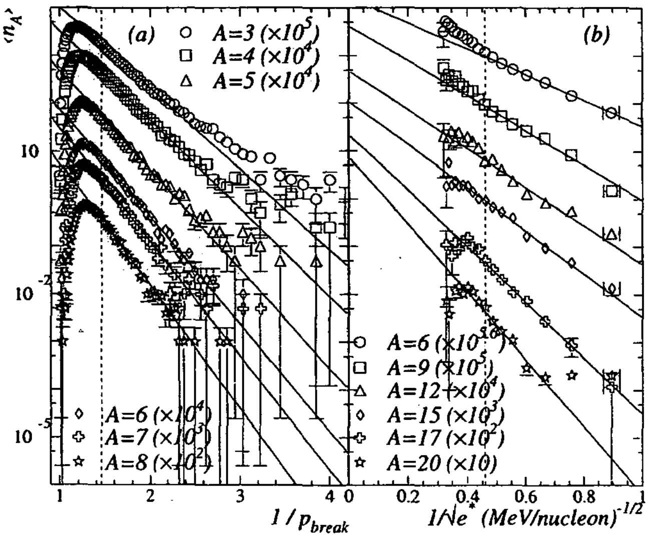

FIG. 4. Normalized average cluster (fragment) multiplicity as a function of $1/p_{break}$ ($1/\sqrt{e^*}$) for clusters (fragments) of different size (mass), A, for percolation (a) (Au multifragmentation (b)). Solid lines show Arrhenius fits. Vertical dashed lines show the location of the critical point.

equal to 0.42 ± 0.02 in agreement with the accepted value of $\sigma = 0.45$ for 3D percolation. See Fig. 5. The constant of proportionality of the power law gives another measure of the surface energy coefficient $c_0 = 2.42 \pm 0.03$.

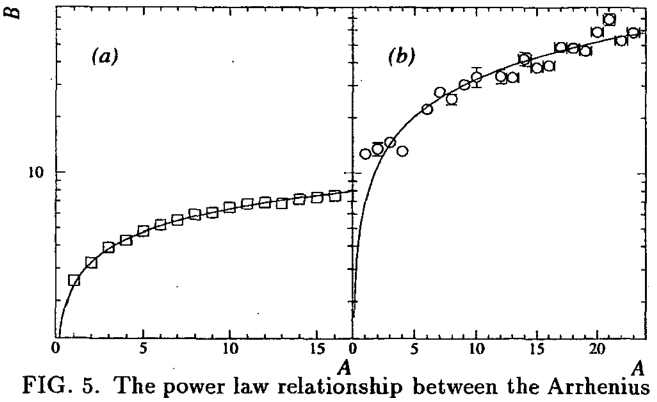

FIG. 5. The power law relationship between the Arrhenius barrier, B, and the cluster size (fragment mass) A for percolation (a) (multifragmentation (b)). The solid line is a fit to the points with $A > 1$.

When the Arrhenius analysis is performed on the Au multifragmentation data, the results are qualitatively similar, but quantitatively distinct. Arrhenius fits of $\ln \langle n_A \rangle$, now plotted against $1/\sqrt{e^*}$, are linear over an order of magnitude or more. See Fig. 4. The barriers extracted here can be converted into units of MeV via the energy-temperature relation for a degenerate Fermi gas. Following the same analysis as for percolation, a fit was made of B vs. A (see Fig. 5) which yielded $\sigma = 0.68 \pm 0.03$, in agreement with previously determined EOS Au multifragmentation values [7], [10], [21] and $c_0 = 6.8 \pm 0.5$ MeV.

In summary, the above effort illustrates:

- the presence of reducibility and thermal scaling in the FDM, percolation and the EOS Au multifragmentation data (the latter two shown empirically);
- the relationship between the FDM and percolation via a scaling analysis that also yields an estimate of the surface energy coefficient;
- that the barriers obtained from percolation follow a power-law dependence on cluster size with an exponent that agrees with the accepted 3D percolation value and gives another (consistent) estimate of the surface energy coefficient;
- the collapse of the EOS Au fragment distributions in accordance with the FDM yielding an estimate of the surface energy coefficient of a low density nuclear system;
- that the barriers obtained from EOS Au multifragmentation data follow a power-law dependence on fragment mass with an exponent near the expected value (2/3) and close to the 3D Ising universality class value (0.64) and gives another (consistent) estimate of the surface energy coefficient.

This work was supported in part by the U.S. Department of Energy and by the National Science Foundation.

---

[1] M. E. Fisher, Physics **3**, 255 (1967).
[2] D. Stauffer and A. Aharony, "Introduction to Percolation Theory", 2nd ed. (Taylor and Francis, London, 1992).
[3] J. E. Finn *et al.*, Phys. Rev. Lett. **49**, 1321 (1982).
[4] X. Campi, Phys. Lett. B **208**, 351 (1988).
[5] W. Bauer *et al.*, Phys. Lett. B 150, **53** (1985).
[6] M. L. Gilkes, *et al.*, Phys. Rev. Lett. **73**, 1590 (1994).
[7] J. B. Elliott *et al.*, Phys. Lett. B, **381**, 24 (1996).
[8] J. A. Hauger *et al.*, Phys. Rev. Lett. **77**, 235 (1996).
[9] J. A. Hauger *et al.*, Phys. Rev. C **57**, 764 (1998).
[10] J. B. Elliott *et al.*, Phys. Lett. B. **418**, 35 (1998).
[11] L. G. Moretto *et al.*, Phys. Rep. **287**, 249 (1997).
[12] L. Beaulieu *et al.*, Phys. Rev. Lett. **81**, 770 (1998).
[13] J. Toke *et al.*, Phys. Rev. C **56**, R1683 (1997).
[14] L. G. Moretto *et al.*, Phys. Rev. C **60**, 031601 (1999).
[15] J. Frenkel, "Kinetic Theory of Liquids", Oxford University Press (1946).
[16] J. E. Mayer and M. G. Mayer, "Statistical Mechanics", John Wiley, New York (1940).
[17] H. Nakanishi and H. E. Stanley, Phys. Rev. B **22**, 2466 (1980).
[18] H. E. Stanely *et al.*, Physica A **266**, 5 (1999).
[19] J. B. Elliott *et al.*, Phys. Rev. C **55**, 1319, (1997).
[20] A. S. Hirsch *et al.*, Phys. Rev. C **29**, 508 (1984).
[21] J. B. Elliott *et al.*, in progress.

ERNEST ORLANDO LAWRENCE BERKELEY NATIONAL LABORATORY
ONE CYCLOTRON ROAD | BERKELEY, CALIFORNIA 94720

Prepared for the U.S. Department of Energy under Contract No. DE-AC03-76SF00098

ABY587
LBL Libraries